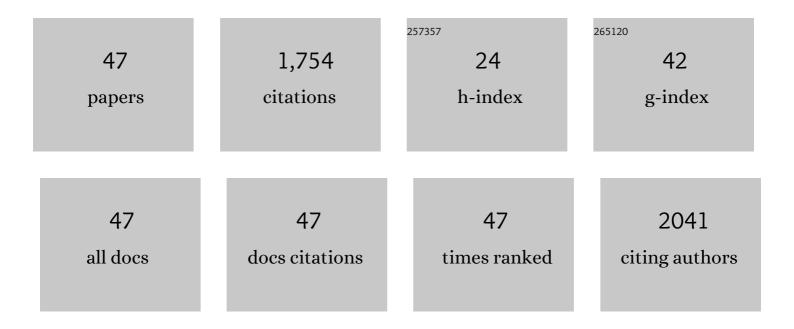
Fengmin Liu

List of Publications by Year in descending order

Source: https://exaly.com/author-pdf/7910208/publications.pdf Version: 2024-02-01



FENCMINLI

#	Article	IF	CITATIONS
1	Nanosheet-Assembled ZnFe ₂ O ₄ Hollow Microspheres for High-Sensitive Acetone Sensor. ACS Applied Materials & Interfaces, 2015, 7, 15414-15421.	4.0	234
2	Double-Shell Architectures of ZnFe ₂ O ₄ Nanosheets on ZnO Hollow Spheres for High-Performance Gas Sensors. ACS Applied Materials & Interfaces, 2015, 7, 17811-17818.	4.0	127
3	Hierarchical flower-like WO3 nanostructures and their gas sensing properties. Sensors and Actuators B: Chemical, 2014, 204, 224-230.	4.0	111
4	Hierarchical Assembly of α-Fe ₂ O ₃ Nanorods on Multiwall Carbon Nanotubes as a High-Performance Sensing Material for Gas Sensors. ACS Applied Materials & Interfaces, 2017, 9, 8919-8928.	4.0	108
5	Ultrasensitive gas sensor based on hollow tungsten trioxide-nickel oxide (WO3-NiO) nanoflowers for fast and selective xylene detection. Journal of Colloid and Interface Science, 2019, 535, 458-468.	5.0	90
6	Mixed potential type acetone sensor using stabilized zirconia and M3V2O8 (M: Zn, Co and Ni) sensing electrode. Sensors and Actuators B: Chemical, 2015, 221, 673-680.	4.0	62
7	Highly Enhanced Sensing Properties for ZnO Nanoparticle-Decorated Round-Edged α-Fe ₂ O ₃ Hexahedrons. ACS Applied Materials & Interfaces, 2015, 7, 8743-8749.	4.0	62
8	Tripartite Layered Photoanode from Hierarchical Anatase TiO ₂ Urchin-Like Spheres and P25: A Candidate for Enhanced Efficiency Dye Sensitized Solar Cells. Journal of Physical Chemistry C, 2013, 117, 24150-24156.	1.5	49
9	Au ₃₉ Rh ₆₁ Alloy Nanocrystal-Decorated W ₁₈ O ₄₉ for Enhanced Detection of <i>n</i> Butanol. ACS Sensors, 2019, 4, 2662-2670.	4.0	47
10	Highly sensitive detection of Pb2+ and Cu2+ based on ZIF-67/MWCNT/Nafion-modified glassy carbon electrode. Analytica Chimica Acta, 2020, 1124, 166-175.	2.6	46
11	Highly sensitive and humidity-independent ethanol sensors based on In ₂ O ₃ nanoflower/SnO ₂ nanoparticle composites. RSC Advances, 2015, 5, 52252-52258.	1.7	42
12	Fabrication of Well-Ordered Three-Phase Boundary with Nanostructure Pore Array for Mixed Potential-Type Zirconia-Based NO ₂ Sensor. ACS Applied Materials & Interfaces, 2016, 8, 16752-16760.	4.0	41
13	High performance mixed-potential type NO2 sensors based on three-dimensional TPB and Co3V2O8 sensing electrode. Sensors and Actuators B: Chemical, 2015, 216, 121-127.	4.0	40
14	Template-free synthesis of novel In2O3 nanostructures and their application to gas sensors. Sensors and Actuators B: Chemical, 2013, 185, 32-38.	4.0	39
15	Gas sensing with hollow α-Fe2O3 urchin-like spheres prepared via template-free hydrothermal synthesis. CrystEngComm, 2012, 14, 8335.	1.3	38
16	Mixed-potential type NO sensor using stabilized zirconia and MoO3–In2O3 nanocomposites. Ceramics International, 2016, 42, 12503-12507.	2.3	37
17	Growth of SnO ₂ nanowire arrays by ultrasonic spray pyrolysis and their gas sensing performance. RSC Advances, 2014, 4, 43429-43435.	1.7	36
18	Gas sensor based on samarium oxide loaded mulberry-shaped tin oxide for highly selective and sub ppm-level acetone detection. Journal of Colloid and Interface Science, 2018, 531, 74-82.	5.0	35

Fengmin Liu

#	Article	IF	CITATIONS
19	Selective-detection NO at room temperature on porous ZnO nanostructure by solid-state synthesis method. Journal of Colloid and Interface Science, 2019, 556, 640-649.	5.0	33
20	Preparation of silver-loaded titanium dioxide hedgehog-like architecture composed of hundreds of nanorods and its fast response to xylene. Journal of Colloid and Interface Science, 2019, 536, 215-223.	5.0	33
21	Sub-ppm YSZ-based mixed potential type acetone sensor utilizing columbite type composite oxide sensing electrode. Sensors and Actuators B: Chemical, 2017, 238, 928-937.	4.0	31
22	Direct growth of NiO films on Al2O3 ceramics by electrochemical deposition and its excellent H2S sensing properties. Sensors and Actuators B: Chemical, 2019, 296, 126619.	4.0	31
23	Facile synthesis and gas-sensing properties of monodisperse α-Fe2O3 discoid crystals. RSC Advances, 2012, 2, 9824.	1.7	29
24	Preparation of Ni(OH) ₂ nanosheets on Ni foam via a direct precipitation method for a highly sensitive non-enzymatic glucose sensor. RSC Advances, 2015, 5, 53665-53670.	1.7	29
25	Synthesis of hierarchical ZnO/ZnFe ₂ O ₄ nanoforests with enhanced gas-sensing performance toward ethanol. CrystEngComm, 2015, 17, 8683-8688.	1.3	24
26	Construction of self-sensitized LiErF4: 0.5% Tm3+@LiYF4 upconversion nanoprobe for trace water sensing. Nano Research, 2020, 13, 2803-2811.	5.8	24
27	Mixed potential type acetone sensor based on GDC used for breath analysis. Sensors and Actuators B: Chemical, 2021, 326, 128846.	4.0	24
28	Controlled synthesis of hierarchical Sn-doped $\hat{I}\pm$ -Fe2O3 with novel sheaf-like architectures and their gas sensing properties. RSC Advances, 2013, 3, 7112.	1.7	23
29	Highly efficiency p-type dye sensitized solar cells based on polygonal star-morphology Cu2O material of photocathodes. Chemical Research in Chinese Universities, 2014, 30, 661-665.	1.3	23
30	Hollow cylinder ZnO/SnO2 nanostructures synthesized by ultrasonic spray pyrolysis and their gas-sensing performance. CrystEngComm, 2014, 16, 6135.	1.3	21
31	Acetone sensing with a mixed potential sensor based on Ce0.8Gd0.2O1.95 solid electrolyte and Sr2MMoO6 (M: Fe, Mg, Ni) sensing electrode. Sensors and Actuators B: Chemical, 2019, 284, 751-758.	4.0	21
32	Triethylamine sensing with a mixed potential sensor based on Ce0.8Gd0.2O1.95 solid electrolyte and La1-xSrxMnO3 (x = 0.1, 0.2, 0.3) sensing electrodes. Sensors and Actuators B: Chemical, 2021, 327, 128830	.4.0	21
33	Monodisperse TiO2 mesoporous spheres with core–shell structure: candidate photoanode materials for enhanced efficiency dye sensitized solar cells. RSC Advances, 2014, 4, 23396.	1.7	18
34	Machine Learning-Assisted Development of Sensitive Electrode Materials for Mixed Potential-Type NO ₂ Gas Sensors. ACS Applied Materials & Interfaces, 2021, 13, 50121-50131.	4.0	16
35	Bimetallic PtRu alloy nanocrystal-functionalized flower-like WO3 for fast detection of xylene. Sensors and Actuators B: Chemical, 2022, 351, 130950.	4.0	16
36	The enhanced CO gas sensing performance of Pd/SnO ₂ hollow sphere sensors under hydrothermal conditions. RSC Advances, 2016, 6, 80455-80461.	1.7	15

Fengmin Liu

#	Article	IF	CITATIONS
37	Enhanced n-pentanol sensing performance by RuCu alloy nanoparticles decorated SnO2 nanoclusters. Sensors and Actuators B: Chemical, 2022, 351, 130900.	4.0	13
38	Novel three-dimensional TiO2 nanomesh synthesized by a one-pot hydrothermal method for application in dye sensitized solar cells. RSC Advances, 2013, 3, 23389.	1.7	11
39	3D TiO ₂ /ZnO composite nanospheres as an excellent electron transport anode for efficient dye-sensitized solar cells. RSC Advances, 2016, 6, 51320-51326.	1.7	11
40	Enhanced photovoltaic properties of dye-sensitized solar cells using three-component CNF/TiO2/Au heterostructure. Journal of Colloid and Interface Science, 2019, 542, 168-176.	5.0	10
41	Highly Selective Mixed Potential Methanol Gas Sensor Based on a Ce _{0.8} Gd _{0.2} O _{1.95} Solid Electrolyte and Au Sensing Electrode. ACS Sensors, 2022, 7, 972-984.	4.0	9
42	Photonic Crystal Effects on Upconversion Enhancement of LiErF ₄ :0.5%Tm ³⁺ @LiYF ₄ for Noncontact Cholesterol Detection. ACS Applied Materials & Interfaces, 2022, 14, 428-438.	4.0	8
43	Understanding the Increasing Trend of Sensor Signal with Decreasing Oxygen Partial Pressure by a Sensing-Reaction Model Based on O ^{2–} Species. ACS Sensors, 2022, 7, 1095-1104.	4.0	7
44	Highly sensitive mixed-potential type ethanol sensors based on stabilized zirconia and ZnNb2O6sensing electrode. RSC Advances, 2016, 6, 27197-27204.	1.7	5
45	Hierarchical TiO2 flower-spheres with large surface area and high scattering ability: an excellent candidate for high efficiency dye sensitized solar cells. Chemical Research in Chinese Universities, 2015, 31, 841-845.	1.3	4
46	Microstructure methane sensor based on Pd-doped SnO <inf>2</inf> nanoparticles. , 2012, , .		0
47	Doping effect of metal oxide on sensing performance of Pd/Al <inf>2</inf> O <inf>3</inf> -based methane sensor. , 2012, , .		Ο